The limits of bioenergy for mitigating global lifecycle greenhouse gas emissions from fossil fuels.

DOI: 10.1038/nenergy.2016.202
Handle: http://hdl.handle.net/1942/23021

Title

The limits of bioenergy for mitigating global lifecycle greenhouse gas emissions from fossil fuels

Authors & affiliation

Mark D. Staples[a]
Robert Malina[a,b]
Steven R. H. Barrett[a,*]

[a] Laboratory for Aviation and the Environment, Department of Aeronautics and Astronautics, Massachusetts Institute of Technology, 77 Massachusetts Avenue, Cambridge, MA 02139
[b] Now at: Center for Environmental Sciences, Hasselt University, Campus Diepenbeek, Agoralaan Building D, 3590 Diepenbeek, Belgium.

[*]Author to whom all correspondence and material should be addressed. Email: sbarrett@mit.edu

Corresponding author

Steven R. H. Barrett
Laboratory for Aviation and the Environment
Department of Aeronautics and Astronautics
Massachusetts Institute of Technology
77 Massachusetts Avenue, Room 33-322, Cambridge, MA 02139
USA
+1 (617) 452-2550
sbarrett@mit.edu

Abstract

In this Article we quantify the optimal allocation and deployment of global bioenergy resources to offset fossil fuels in 2050. We find that bioenergy could reduce lifecycle emissions attributable to combustion-fired electricity and heat, and liquid transportation fuels, by a maximum of 4.9-38.7 Gt CO_2e, or 9-68%, and that offsetting fossil fuel-fired electricity and heat with bioenergy is on average 1.6-3.9 times more effective for emissions mitigation than offsetting fossil fuel-derived liquid fuel. However, liquid fuels make up 18-49% of global optimally allocated final bioenergy in our results for 2050. This indicates that a mix of bioenergy end-uses maximizes lifecycle emissions reductions. Finally, our findings demonstrate that emissions reductions are maximized by limiting deployment of total available primary bioenergy to 29-91%, and that lifecycle emissions are a constraint on the usefulness of bioenergy for mitigating global climate change.

Main text

The use of modern bioenergy is motivated by regionally- and context-dependent factors, including: the desire for domestically-sourced, secure, and diverse energy systems; the promotion of rural economic development; the renewable nature of biomass; and the potential to mitigate anthropogenic greenhouse gas (GHG) emissions by offsetting demand for fossil fuels [1,2]. In contrast to fossil fuels, carbon dioxide (CO_2) emissions from the combustion of biomass or biomass-derived fuels are biogenic, meaning that carbon in the fuel comes from atmospheric CO_2 recently sequestered during photosynthesis. This is used to justify accounting guidelines for CO_2 from bioenergy, whereby combustion emissions are assumed to be offset by sequestration during biomass growth [3].

However, there are GHG emissions associated with the cultivation, transportation, and conversion of bioenergy to final energy products, and lifecycle analysis (LCA) is employed to quantify these emissions. For example, the Greenhouse Gases, Regulated Emissions, and Energy Use in Transportation (GREET) model, among others, has been used to quantify the lifecycle (LC) 100-year global warming potential (GWP_{100}) CO_2-equivalent (CO_2e) emissions attributable to biomass- and fossil fuel-derived transportation fuels [4-10], electricity, heat and other energy carriers [10-12]. In addition, consequential LCA has been used to estimate the aggregate change in emissions to the environment due to specific policies or actions by employing partial- and general-equilibrium economic models of the market-mediated impacts of bioenergy use. A number of studies have demonstrated the importance of consequential LC emissions associated with the large-scale adoption of bioenergy, specifically the contribution of CO_2 emissions from land use change (LUC) [13-15].

A large body of work has also quantified the size of the global bioenergy resource. Early work focused on estimating the land area available for cultivation and future biomass productivity, finding that many hundreds of exajoules of primary bioenergy are potentially available annually [16,17]. Subsequent studies have quantified bioenergy potentials that are cost-effective, avoid competition with food or feed production, or limit the environmental impacts of large-scale adoption [18-20]. Generally, these additional considerations result in lower estimates of primary bioenergy potential, on the order of ~100 EJ/yr.

Despite these advances, significant uncertainties remain in the literature regarding the determinants of global bioenergy availability. For example, a recent review of 90 studies indicates that by mid-century bioenergy crops, forestry, residues, and wastes could satisfy ~100-600 EJ of annual global primary energy demand [21] (the International Energy Agency (IEA) estimates that 2050 primary energy demand will be 681-929 EJ [22]), and that the broad range of results is driven primarily by assumptions regarding future demand for food, agricultural productivity gains, and the availability of land for energy crop cultivation. Although this continues to be an active area of research, to the best of our knowledge no peer-reviewed analysis to date has quantified the potential for bioenergy to contribute to anthropogenic GHG emissions reductions, accounting for both the limits of bioenergy availability and LC emissions including LUC.

In this Article, we present a model of future land availability, areal bioenergy yields, and LC emissions including LUC, to establish the relationship between global availability of bioenergy and the potential for GHG emissions reductions. Our hypothesis is that the use of bioenergy for GHG emissions mitigation is constrained not only by growth in biomass productivity and the availability of land for energy crop cultivation in the future [21], but also by the LC emissions of final energy derived from biomass relative to the fossil fuels that bioenergy would replace. We

test this hypothesis by quantifying the optimal allocation and deployment of bioenergy resources to maximize reductions in LC GHG emissions in 2050. The findings represent an estimate of the limits of the GHG mitigation potential of bioenergy, and of the degree to which bioenergy can contribute to climate stabilization goals by mid-century.

Primary bioenergy availability and land requirements

Projections of land available for biomass cultivation, energy crop yields, and residue and waste generation, are used to quantify the potential future global availability of primary bioenergy, and the results are compared to existing studies to validate our approach. Table 1 shows the calculated values for primary bioenergy and required land area for three scenarios in 2050: low, mid and high bioenergy availability. We calculate a range of 112-794 EJ/yr of primary bioenergy, requiring 634-2807 Mha of land for biomass cultivation. For context, global oilseed and maize harvested areas were 291 Mha and 186 Mha, respectively, and total global arable agricultural land area was 1408 Mha, in 2013 [23]. These results are consistent with the recent meta-analysis by Slade, Bauen & Gross (2014), and the low and mid scenarios are within the envelope of estimates defined by those authors as 'plausible' (between 100 EJ/yr requiring <500Mha land area, and 600 EJ/yr requiring >1500 Mha land area) [21].

We also disaggregate the results in Table 1 by energy crops, and residue and waste feedstocks. The land areas required for energy crop cultivation imply average areal biomass yields that are congruent with the literature (8.1-13.7 oven dry tonnes (odt)/ha, assuming a lower heating value (LHV) of 18 GJ/odt) [21]. The calculated availability of primary bioenergy from residue and waste is 19-101 EJ/yr, which also agrees with previous analyses: Daioglou et al. (2015) projected global residue availability of 48 EJ/yr by 2050, and reported estimates of 20-86 EJ/yr from similar peer-reviewed studies [24].

Table 1: **Results of 2050 primary bioenergy availability scenarios**

Bioenergy availability scenario	**Low**		**Mid**		**High**	
	Primary energy [EJ/yr]	**Land [Mha]**	**Primary energy [EJ/yr]**	**Land [Mha]**	**Primary energy [EJ/yr]**	**Land [Mha]**
Vegetable oil energy crops	17	216	43	500	32	688
Sugary & starchy energy crops	33	204	60	498	100	802
Lignocellulosic energy crops	43	214	210	664	561	1317
Energy crop subtotal	93	634	312	1662	693	2807
Agricultural residues	15	-	46	-	81	-
Forestry residues	4	-	9	-	19	-
Waste fats, oils & greases (FOG)	1	-	1	-	1	-
Residue & waste subtotal	19	-	56	-	101	-
Total	**112**	**634**	**368**	**1662**	**794**	**2807**

In order to identify the parameters driving variability between the low, mid, and high scenarios, a sensitivity analysis of primary bioenergy availability is carried out. We find that the three variables contributing to the greatest variation from the mid scenario results are: the minimum threshold for agro-climatic suitability of lands for energy crop cultivation; growth in energy crop yields; and the assumed 2050 land use scenario. These parameters are further explained in the Methods section and Supplementary Table 10, and the results are presented in Supplementary Figure 3.

Optimal bioenergy allocation and deployment

Based on the primary bioenergy results above, we establish curves of final bioenergy availability from four competing end-uses (middle and heavy distillate fuels; light distillate fuels; heat; and electricity), versus specific LC emissions including location- and pathway-specific LUC emissions. The optimal allocation of each unit of available primary bioenergy amongst these four mutually exclusive end-uses is determined using the iterative optimization routine which maximizes total LC GHG emissions reductions compared to fossil fuels (see Equation 1 in the Methods section). We note that biomass resources could also be allocated to end-uses beyond those studied here in order to mitigate GHG emissions, such as bio-chemicals or the use of plant-based foods to offset demand for livestock production. However, this analysis focuses on these four end uses because energy-related emissions make up approximately 68% of total annual anthropogenic GHG emissions [25].

The resulting curves of final bioenergy availability and specific LC emissions are shown in Figure 1, broken out by middle and heavy distillate fuels, light distillate fuels, heat, and electricity, for each of the three bioenergy availability scenarios. The curves consist of discrete units of available final bioenergy, rank-ordered from lowest to highest specific LC emissions (gCO_2e per $MJ_{final\ energy}$), with LC emissions per unit of final bioenergy monotonically increasing with greater final bioenergy deployment. The four uses of final bioenergy shown in Figure 1 (middle and heavy distillate fuels; light distillate fuels; heat; and electricity) have non-LUC LC emissions ranging from 5.5-39.1, 5.5-50.4, 7.3-13.8, and 12.8-27.5 $gCO_2e/MJ_{final\ energy}$, respectively. The share of LC emissions above these values corresponds to the contribution of LUC emissions for a given unit of biomass-derived final energy, and therefore LUC accounts for a greater proportion of total LC emissions from final bioenergy moving to the right along the colored curves. The horizontal sections of the curves reflect final energy derived from residue and waste feedstocks, for which specific LC emissions are constant because there are no associated LUC emissions. Pathway-specific non-LUC LC emissions data are available in Supplementary Table 11.

The final bioenergy results are compared to three scenarios of projected 2050 global demand for combustion-generated electricity and heat and liquid transportation fuels, derived from fossil fuels, shown in black and adapted from the 2°C, 4°C and 6°C temperature change scenarios (2DS, 4DS and 6DS) of the IEA Energy Technology Perspectives (ETP) 2014 report and database [22]. These curves are rank-ordered in terms of decreasing specific LC emissions, with LC emissions per unit of fossil fuel-derived final energy monotonically decreasing with greater deployment of bioenergy to offset fossil fuel demand.

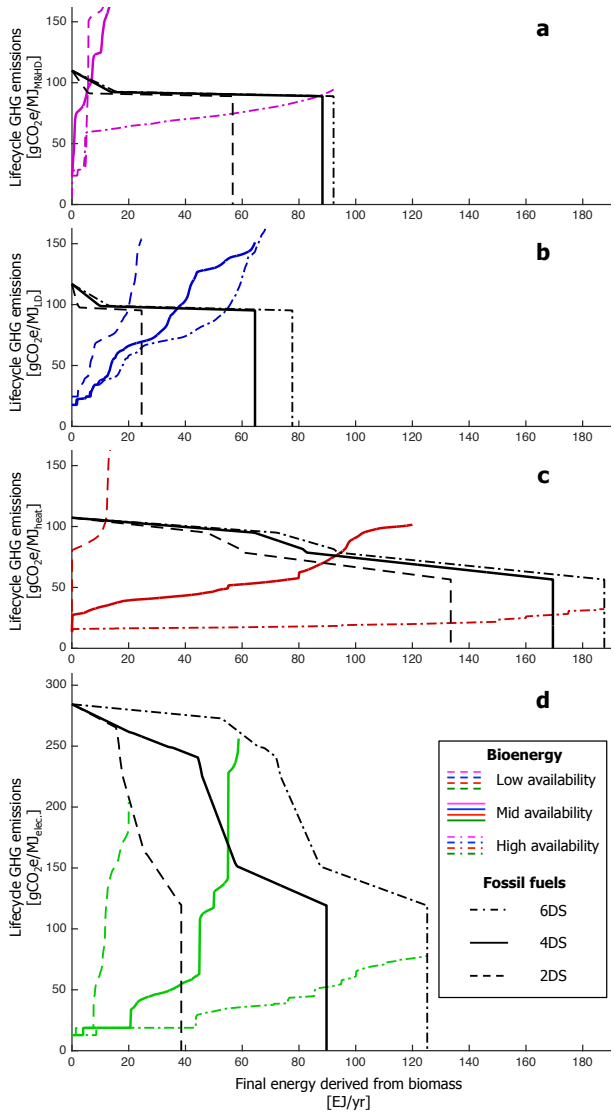

Figure 1: Availability and specific LC GHG emissions of optimally allocated final bioenergy compared to fossil fuel-derived final energy demand and emissions in 2050. Panel a shows biomass-derived (magenta) and petroleum-derived (black) middle and heavy distillate (M&HD) liquid fuels. Panel b shows biomass-derived (blue) and petroleum-derived (black) light distillate (LD) liquid fuels. Panel c shows biomass-derived heat final energy (red), compared to coal-, oil-, and natural gas-derived heat (black). Panel d shows biomass-derived electricity (green), compared to for coal-, oil-, and natural gas-derived electricity (black). The colored bioenergy curves in each panel correspond to the three bioenergy availability scenarios, and the black fossil fuel curves correspond to the 2°C, 4°C and 6°C temperature change scenarios (degree scenarios, DS) from IEA ETP [22]. Further information on the definition of these curves is found in the Methods section.

The results shown in Figure 1 are used to compare the specific LC emissions of optimally allocated biomass-derived final energy to its fossil fuel analog at a given level of bioenergy deployment. By doing so, the change in LC emissions from offsetting the marginal unit of fossil fuel with the marginal unit of bioenergy can be determined. This implies that, for any given pairing of bioenergy and fossil fuel curves for each of the end-uses shown in Figure 1, bioenergy deployment beyond the point of intersection of the two curves represents a net increase in LC emissions. Therefore, we define the optimal level of bioenergy deployment to offset fossil fuel demand as the point of intersection of two curves, where the LC emissions of the bioenergy and fossil fuel pathways are equivalent and the total reduction in GHG emissions (the area between the curves in Figure 1) is maximized.

Figure 2 shows final bioenergy deployment plotted against cumulative mitigation of GHG emissions, calculated as the integrated area between the curves from Figure 1. The results are disaggregated by bioenergy end-use, the optimal levels of deployment for each being maxima of their corresponding curves. The results for each end-use are stacked in order to indicate total optimal final bioenergy deployment and the associated maximum reduction in GHG emissions. The results are calculated for all nine combinations of bioenergy and fossil fuel curves (shown in Table 2), and three scenarios are shown in Figure 2 to represent a broad range of the optimal final bioenergy deployment (57-460 EJ/yr), and maximum GHG emissions reduction (4.9-38.7 Gt_{CO2e}/yr) results. The results of the mid bioenergy availability and 4DS scenario combination indicate an optimal final bioenergy deployment of 192 EJ/yr, leading to GHG emissions reductions of 17.2 Gt_{CO2e}/yr. The three scenarios correspond to 88, 273 and 721 EJ/yr of primary bioenergy deployment in the low, mid and high bioenergy availability scenarios.

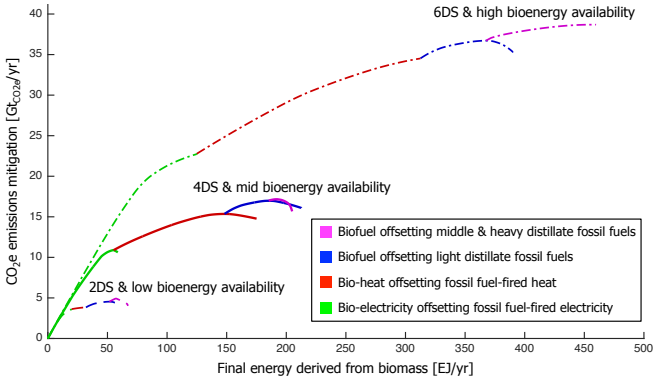

Figure 2: Deployment of biomass-derived final energy versus cumulative GHG emissions mitigation. The maximum of each curve represents the optimal level of final bioenergy deployment for the indicated final energy end-use. The dashed line denotes the combination of the 2DS fossil fuel and low bioenergy availability scenarios, the solid line denotes the combination of the 4DS and mid bioenergy availability scenarios, and the dash-dot line denotes the combination of the 6DS and high bioenergy availability scenarios..

Table 2 shows tabular results for all nine scenario combinations, compared to total primary bioenergy availability, global final energy demand for combustion-generated electricity and heat, and liquid transportation fuels, and the total associated LC emissions if this demand were to be satisfied completely with fossil fuels. This comparison indicates that optimal bioenergy deployment could satisfy 10-97% of projected 2050 final energy demand for fossil fuel-derived electricity, heat, and liquid fuels, corresponding to a reduction in GHG emissions from these sources of 9-68%. This coincides with deployment of 29-91% of the total available primary bioenergy reported in Table 1. In the mid bioenergy availability and 4DS scenario combination, optimal final bioenergy deployment is 47% of final energy demand for electricity, heat, and liquid fuels, requiring 74% of available primary bioenergy, and resulting in a 36% reduction in LC emissions.

Table 2: **Optimal bioenergy allocation and associated maximum GHG emission reductions.** Primary bioenergy availability, final bioenergy deployment, and the reduction in LC GHG emissions are compared against 2050 final energy demand for combustion-generated electricity and heat, and liquid transportation fuels from fossil fuels, and the associated LC GHG emissions.

2050 scenario					Optimal bioenergy deployment													
Global demand for fossil fuel elec., heat, and liquid transp. fuels		LC GHG emissions from fossil fuels	Primary bioenergy avail.		Primary energy		Final energy						Maximum GHG emissions reduction					
					Total	Propoortion of total avail.	Elec.	Heat	LD fuels	M&HD fuels	Total	Offset of final energy demand	Elec.	Heat	LD fuels	M&HD fuels	Total	Reduction in LC GHG emissions
[EJ/yr]		[Gt_{CO2e}/yr]	[EJ/yr]		[EJ/yr]	[%]	[EJ/yr]					[%]	[Gt_{CO2e}/yr]					[%]
			Low	112	88	79%	20	12	20	5	57	22%	3.6	0.2	0.7	0.4	4.9	18%
2DS	253	26.8	Mid	368	239	65%	35	121	25	8	188	74%	5.8	5.9	1.1	0.4	13.3	49%
			High	794	230	29%	23	134	25	14	195	77%	5.5	8.8	1.3	0.7	16.4	61%
			Low	112	90	80%	26	0	25	0	51	12%	4.0	0.0	1.2	0.0	5.2	11%
4DS	412	47.1	Mid	368	273	74%	55	93	37	7	192	47%	10.9	4.5	1.6	0.2	17.2	36%
			High	794	613	77%	90	170	54	88	401	97%	15.6	11.1	2.1	3.3	32.2	68%
			Low	112	89	79%	26	0	24	1	50	10%	4.4	0.0	1.2	0.0	5.6	9%
6DS	483	59.6	Mid	368	286	78%	75	62	37	7	181	37%	15.8	2.3	1.7	0.2	19.9	33%
			High	794	721	91%	125	188	55	92	460	95%	22.8	11.8	2.2	2.0	38.7	65%

GHG mitigation effectiveness and mix of bioenergy end-uses

In order to compare between the different bioenergy end-uses considered in this analysis, average GHG mitigation effectiveness is defined as the ratio of maximum GHG emissions reduction to total optimal final bioenergy deployment. This is shown in Table 3, broken out by all four bioenergy end-uses, as well as aggregated to biomass-fired electricity and heat, and liquid biofuels. In the nine scenario combinations, the average GHG mitigation effectiveness of biomass-fired electricity and heat, and liquid biofuels, range from 0.08-0.17 Gt_{CO2e}/EJ and 0.03-0.05 Gt_{CO2e}/EJ, respectively. The average GHG mitigation effectiveness of biomass-fired electricity and heat is 1.6-3.9 times higher than that of liquid biofuels across all scenario combinations. This indicates that, from a GHG mitigation perspective, biomass combustion to generate electricity or heat is, in aggregate, a more effective end-use for bioenergy resources than liquid biofuel production. This is in line with previous studies that identify power and heat generation as a more environmentally beneficial use of scarce biomass resources than the production of liquid fuels [26-30].

Table 3: **Average GHG mitigation effectiveness of bioenergy end-uses in 2050**. This is defined as the ratio of maximum GHG emissions reduction, and total final energy, from biomass-derived electricity, heat, light distillate (LD) fuels, and middle & heavy distillate (M&HD) fuels.. The ratio of effectiveness of electricity and heat to liquid fuels is shown in the rightmost column.

Fossil fuel scenario	Bioenergy availability	Average effectiveness [Gt_{CO2e}/EJ]						Ratio of elec. & heat to liquid fuels effectiveness
		Elec.	Heat	Biomass-fired elec. & heat	LD fuels	M&HD fuels	All liquid biofuels	
2DS	Low	0.18	0.02	0.12	0.04	0.07	0.04	2.7
	Mid	0.17	0.05	0.08	0.04	0.05	0.05	1.6
	High	0.24	0.07	0.09	0.05	0.05	0.05	1.7
4DS	Low	0.16	-	0.16	0.05	0.02	0.05	3.3
	Mid	0.20	0.05	0.10	0.04	0.03	0.04	2.5
	High	0.17	0.07	0.10	0.04	0.04	0.04	2.7
6DS	Low	0.17	-	0.17	0.05	0.02	0.05	3.4
	Mid	0.21	0.04	0.13	0.04	0.03	0.04	3.1
	High	0.18	0.06	0.11	0.04	0.02	0.03	3.9

Despite having a lower average GHG mitigation effectiveness, however, 18-49% of the calculated total optimal final bioenergy comes from liquid biofuels in all scenarios investigated. The reason for this can be observed in Figure 2. The initial marginal effectiveness (or slopes) of offsetting fossil fuel-fired electricity and heat with bioenergy (the beginning of the green and red curves) is greater than that of offsetting petroleum-derived liquid fuels (the beginning of the blue

and magenta curves). This indicates that, initially, biomass-fired electricity and heat production maximizes GHG emission reductions per unit of final bioenergy. However, as the level of deployment of these bioenergy end-uses increases along the curves, the marginal effectiveness of offsetting electricity and heat decreases and eventually becomes equivalent to the initial marginal effectiveness of offsetting petroleum-derived liquid fuels. Beyond this point a switch occurs between competing bioenergy end-uses, and using the next unit of final bioenergy to offset petroleum-derived fuels maximizes GHG emissions reductions. This is because the fossil fuel-fired electricity and heat with the highest specific LC emissions has already been offset, and the greatest subsequent reduction in GHG emissions can be achieved by using liquid biofuels to offset petroleum-derived fuels with relatively high specific LC emissions.

This finding is particularly relevant for sectors with few technical options beyond the use of bioenergy to reduce GHG emissions, but where the use of scarce bioenergy resources may not be justified as the most effective among competing end-uses. One such example is the aviation industry, for which it is technically infeasible to make use of other forms of renewable energy or vehicle electrification, and will therefore require the use of energy-dense liquid fuels (potentially including biomass-derived fuels) for the foreseeable future [31-34]. At the same time, Trivedi et al. (2015) demonstrate that using lignocellulosic feedstocks to produce drop-in middle distillate fuels (including jet fuel) is less societally beneficial than alternative bioenergy uses on average [26].

In contrast, our analysis shows that an optimal deployment of bioenergy resources to maximize GHG reductions requires a mix of bioenergy end-uses. Notably, this mix consists of uses that are not necessarily the most effective, initially or on average, including drop-in middle distillate fuels such as jet fuel. Note that we have only considered renewable ethanol, gasoline, and diesel pathways as representative proxies in this analysis, and that these fuels are not suited for use in aviation [35]. However, a number of technologies exist to convert biomass to renewable jet fuel, with feedstock-to-fuel conversion efficiencies and LC emissions comparable to the pathways that we have considered here [7, 9, 36-41].

LUC emissions amortization and payback period

LUC emissions are included in total LC emissions by amortizing evenly over a 30-year time horizon without discounting, consistent with the United States Environmental Protection Agency (US EPA) approach to assessment of LUC emissions from biofuel production [42]. To test the sensitivity of the findings to this assumption, results are also generated for a 20-year amortization period, consistent with the European Union Renewable Energy Directive [43]. These results are available in Supplementary Note 6, and the maximum GHG emissions reductions are 5-26% smaller than those calculated when assuming a 30-year amortization period.

Alternatively, the payback period can be calculated for LUC emissions associated with a given unit of final bioenergy. This is shown aggregated for all four end-uses in Figure 3. LUC is assumed to result in a one-time pulse of CO_2 emissions, and the payback period is defined as the number of years required for the difference in the LC emissions of a unit of final bioenergy (excluding LUC emissions) and its fossil fuel analog to make up for the LUC emissions pulse. The payback period of the last unit of final bioenergy deployment is shown as a function of cumulative final bioenergy deployment in Figure 3, for the three scenarios combinations of bioenergy and fossil fuel curves from Figure 2. The calculated LUC emissions payback increases with increasing bioenergy deployment up to 39, 35 and 31 years for optimal final bioenergy deployment in the low bioenergy availability and 2DS, mid bioenergy availability and 4DS, and high bioenergy availability and 6DS scenario combinations, respectively. The end point of each

curve represents the level of optimal final bioenergy deployment, and corresponding payback period, for each scenario combination.

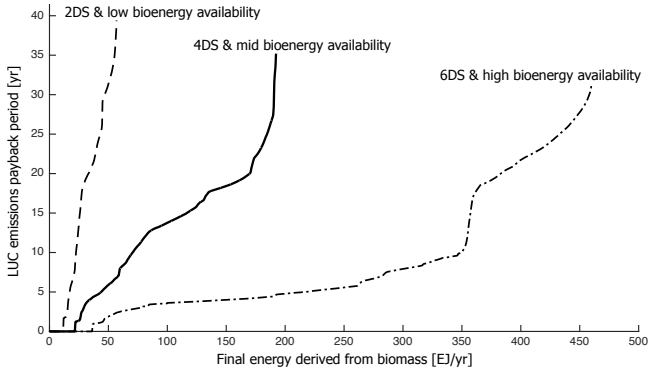

Figure 3: Deployment of biomass-derived final energy versus payback period for LUC emissions. The end point of each curve in the figure represents the optimal level of final bioenergy deployment for that scenario combination of bioenergy and fossil fuel curves.

Limitations and areas for future research

Several additional factors could impact the results that have been calculated here. For example, energy crop cultivation is considered only on lands where irrigation is not a prerequisite for agro-climatic suitability, and potentially disruptive innovations in biomass cultivation, such as the intensification of agricultural production using multi- or intercropping, are not captured in the results presented above [44]. These assumptions could result in an underestimate of agricultural production at the intensive margin. In order to quantify the magnitude of the potential for intensification, a sensitivity analysis is carried out for the three scenarios shown in Figure 2, where the land requirements of bioenergy cultivation are reduced by 50%. This assumption implies that for each unit of biomass cultivated on new land brought into agricultural production, a second unit of comes from intensified production on existing agricultural lands. The result is an increased proportion of fossil fuel final energy demand offset by bioenergy, from between 22-95% to 48-96% for the three scenarios considered. Correspondingly, the range of reductions in LC GHG emissions from electricity, heat and liquid fuels grows from between 18-65%, to 39-76%. These results are available in Supplementary Note 7. Although this is a simplified example for the purposes of sensitivity analysis, the results demonstrate the potential importance of intensification for the GHG emissions mitigation potential of bioenergy.

Industrial aquaculture of feedstocks, such as algae, could represent a large additional source of primary bioenergy because they are not limited by the availability of land area for cultivation and the associated LC emissions impact of LUC. In practice, the production potential of these feedstocks is constrained by local availability of solar insolation, concentrated CO_2, and water as a growth medium, among other factors [45]. Consideration of these parameters is beyond the scope of the work presented here, however future work in this field would benefit from the inclusion of aquaculture feedstocks, focusing on the LC emissions tradeoffs between total feedstock production potential and appropriate siting of cultivation facilities.

A lack of regionally specific data for 2050 necessitates a simplified approach for quantifying the LC emissions of fossil fuel and biomass-derived final energy: this analysis adopts point estimates of LC emissions to represent 35 biomass feedstock-to-final energy conversion pathways, and 24 fossil fuel-derived final energy carriers. In reality, the range of LC emissions of different energy sources exist on a location-dependent continuum that is not fully represented here. Furthermore,

the large-scale use of emerging feedstock-to-final energy technologies that are not considered in this work could offer greater opportunities for GHG emissions mitigation, or even net sequestration, such as electricity generation from biomass coupled with carbon capture and storage (CCS) [46-48]. We note that a more complete global assessment of the GHG mitigation potential of bioenergy could build upon the work presented here by accounting for technological development, and regional and temporal heterogeneity in LC emissions, as reliable data becomes available. In addition, inclusion of the use of bioenergy to offset additional sources of GHG emissions, such as chemicals manufacturing from fossil fuels, or livestock production, would improve the calculation of optimal final bioenergy deployment.

There are also economic feedbacks associated with bioenergy deployment and availability that could be the subject of future research. For example, the valorization of waste and residues might drive up their commodity prices, such that these feedstocks are no longer considered wastes and residues. This could influence the allocation of resources, production patterns, and ultimately feedstock availability. However, the focus of this work is the physical limits of global LC emissions reductions from the use of bioenergy, and therefore the economic impacts and feedbacks described above have not been captured here.

Finally, we note that GWP_{100} has been used as the *de facto* standard for LCA climate metrics in the past, including in GREET1 2015 and in this analysis. Future work in this area could benefit from the use of alternative metrics. For example, a metric that reflects physical impacts, such as global temperature potential (GTP), may be more relevant for policy-making [49]. In addition, accounting for LUC emissions in the context of LCA requires comparison of an emissions pulse at time zero to other LC emissions in subsequent time steps. Therefore, a dynamic metric that reflects the physical processes of climate change, such as annual radiative forcing (RF) impact, would more accurately account for the time-dependent emissions profiles of large-scale bioenergy deployment.

Discussion

The range of optimal final bioenergy deployment calculated in this analysis represents 10-97% of projected annual demand for combustion-generated electricity and heat, and liquid transportation fuels in 2050, across the nine scenarios considered. This corresponds to a reduction in annual LC GHG emissions from these sources of 9-68%, if this demand were otherwise satisfied with fossil fuels. We note that each of the scenarios reported here reflects a different state of the world in 2050 in terms of two distinct but interdependent domains: the availability and allocation of primary bioenergy resources amongst competing end uses; and the types and quantities of fossil fuels used to satisfy final energy demand. These scenarios are defined in order to capture the limits of GHG emissions mitigation potential from bioenergy under a range of potential future conditions, and we do not claim there is predictive or probabilistic meaning to any specific scenario combination over the others.

It is important to highlight that this analysis minimizes GHG emissions by assuming that the next available unit of bioenergy is used for the lowest LC emissions intensity end-use, and to offset the highest LC emissions intensity unit of final fossil fuel energy. This implies a frictionless matching of final bioenergy supply to the fossil fuel use that will result in the greatest reduction in GHG emissions globally, without incurring additional LC emissions from transportation or transmission. This is a simplifying assumption, and therefore the results should be interpreted as an upper bound on GHG mitigation potential via the uses of bioenergy considered here to 2050. In reality, decisions about bioenergy resource allocation, fossil fuel use, and land use planning are not made solely on the basis of GHG emissions. Practical limitations that are not represented

here, such as existing investments in fossil fuel resources and infrastructure, the challenges of biomass transportation logistics, path dependency of energy and environmental policy, economic considerations, and other factors, will guide decisions about bioenergy deployment and the sources of energy it will replace or offset in the future. These factors are beyond the scope of our analysis; however, they represent additional constraints on bioenergy adoption, and on the potential reductions in GHG emissions that have been calculated in this analysis.

In summary, we quantify the optimal allocation and deployment of bioenergy resources to mitigate GHG emissions from fossil fuel-fired electricity and heat, and petroleum-derived liquid transportation fuels, to 2050. The findings provide evidence for the hypothesis that GHG emissions mitigation via the use of bioenergy is constrained not only by the availability of biomass, as considered in previous assessments of bioenergy potential, but also by the LC emissions of final bioenergy when LUC is taken into account: we find that GHG emissions reductions are maximized when deployment is limited to 29-91% of total primary bioenergy availability. In addition, the results show that while biomass-fired electricity and heat generation are, on average, more effective means of GHG mitigation than the production of biomass-derived liquid fuels, optimal bioenergy use requires a mix of end-uses to maximize GHG reductions.

Methods

Primary bioenergy availability

The potential availability of energy crops in 2050 is quantified by using data from three sources: Food and Agriculture Organization of the United Nations, Statistics Division (FAOSTAT) data is used to project future average energy crop yields [50]; maximum agro-climatically attainable yields from the Global Agro-ecological Zones Model (GAEZ) are scaled to reflect geo-spatial heterogeneity in crop yields, and to provide a theoretical upper bound on areal yields of above ground biomass [51]; and the Land Use Harmonization (LUH) database is used to estimate land availability for energy crop cultivation in 2050 [52]. In addition, we calculate emissions from land use change (LUC) to establish energy crops on forestland and pastureland by using 100 cm soil and biomass carbon stock data developed for Global Trade Analysis Project (GTAP) Agro-ecological Zones Emissions Factor (AEZ-EF) database [53]. Combining these sources, we generate a database of energy crop production potential and associated LUC emissions in 2050 from starchy, sugary, vegetable oil and lignocellulosic energy crops, globally resolved at 0.083°. This analysis does not explicitly consider primary bioenergy availability from forestry (other than residues), however the potential availability of bioenergy from the establishment of energy crop cultivation (including lignocellulosic crops) on forestlands is included. Additional information is in Supplementary Note 1.

Primary bioenergy from crop residues is calculated from the potential availability of energy crops, as described above, coupled with a range of food crop production projections that reflect the Intergovernmental Panel on Climate Change (IPCC) Fifth Assessment Report (AR5) Shared Socio-economic Pathways (SSP) [54]. Residue to primary crop ratios are estimated from Lal (2005), and a range of net residue availability of 14.0% to 47.5% is assumed [55-58]. Additional information is in Supplementary Note 2.

The availability of primary energy from forestry residues is quantified from estimates of industrial roundwood and woodfuel production in 2050 [59], combined with estimates of the net availability of logging and wood processing residues that range from 8.0% to 35.5% and 1.0% to 26.3%, respectively [58-60]. Additional information is in Supplementary Note 2.

The availability of waste fats, oils and greases (FOG) is estimated from livestock production projections scaled to the SSP scenarios [61], together with a range of estimates of livestock species-specific net waste FOG availability [62-64]. Additional information is in Supplementary Note 2.

In order to capture variability in the underlying assumptions, three scenarios (low, mid, and high) are defined for the availability of primary bioenergy in 2050. The parameter assumptions that correspond to the scenario definitions can be found in Supplementary Table 10 in Supplementary Note 3, and detailed information about the feedstock scope and modeling of primary bioenergy availability can be found in Supplementary Note 1.

Final bioenergy availability & associated lifecycle emissions

The availability of final energy derived from biomass, and the associated LC emissions per unit of final energy, is calculated by considering four potential end-uses for bioenergy: biomass combustion for electricity generation; biomass combustion for heat generation; production of renewable liquid fuels interchangeable with light distillate petroleum-derived fuels (such as ethanol or renewable gasoline); and production of renewable liquid fuels interchangeable with middle and heavy distillate petroleum-derived fuels (such as renewable diesel). In order to capture these different feedstock end-uses, 35 representative feedstock-to-final energy carrier pathways are selected. The feedstock-to-final energy carrier conversion efficiencies, attributional LC emissions factors, and energy allocation factors for LUC emissions associated with each conversion pathway, are derived from the GREET1 2015 database in terms of grams of GWP_{100} CO_2e per MJ of final energy, as defined in the IPCC AR5 [49]. This data is available in Supplementary Note 4. LUC emissions associated with the establishment of energy crop cultivation on pastureland and forestland are also accounted for using the GTAP AEZ-EF database [50]. Note that, because each unit of energy crop cultivation is assumed to be additional to other projected land uses in 2050, all primary bioenergy availability from energy crops requires the extensification of cultivated land in the context of this analysis, and is therefore associated with some degree of LUC emissions. The sensitivity of our results to this assumption is quantified in Supplementary Note 7.

Fossil fuel-derived final energy & associated lifecycle emissions

The horizontal dimension of the fossil fuel curves shown in Figure 1 reflect projected 2050 demands for middle and heavy distillate liquid fuels, light distillate liquid fuels, combustion-generated heat, and combustion-generated electricity, in panels a-d, respectively. 2050 projected demands are derived from the 2DS, 4DS and 6DS scenarios from the IEA (2014) report and database [22]. The IEA ETP scenarios reflect three possible futures for the energy system in 2050, resulting in projected mean global temperature changes of 2°C, 4°C and 6°C by 2100. IEA (2014) [22] and GREET1 2015 data are used to estimate the mix of fossil fuels for 2050 projected demands that defines the vertical dimension of the fossil fuel curves in Figure 1, specific LC emissions [65]. The ranges of specific LC emissions in the fossil fuel-derived liquid fuel curves (panels a and b) reflect the projected proportions of global conventional and unconventional crude oil production in 2050 [66]. The range of LC emissions in the fossil fuel-fired heat and electricity curves (panels c and d) reflect the projected mix of heat and electricity generation from coal, oil and natural gas, as well as the range of thermal efficiencies of generation technologies used with those fuels [22]. Additional information on the definition of these curves is provided in Supplementary Note 5.

Maximization of GHG emissions mitigation

In cases where multiple energy crop types could potentially be grown on the same parcel of land, the feedstock and conversion pathway that results in the greatest annual reduction in GHG emissions is selected, taking into account the LC and LUC emissions associated with the bioenergy pathway, as well as the LC emissions of the unit of fossil fuel analog that would be offset. For a given original land use type k in each 0.083° grid cell g, the maximum reduction in GHG emissions $R_n(k,g)$ via bioenergy pathway n is defined by Equation 1.

Equation 1

$$R_n(k,g) = \max_{n \in [N]} \left\{ \left[LC_{fossil}(n) \cdot y(n) \cdot c(n) \cdot a(k) \right] - \left[\left(LC_{bio}(n) \cdot y(n) \cdot c(n) \cdot a(k) \right) + \left(\frac{\omega(n) \cdot LUC(k) \cdot a(k)}{m} \right) \right] \right\},$$

where

$R_n(k,g)$ = max. GHG emissions reduction on land type k (pasture or forestland) in cell g [gCO_2e/yr]

$[N]$ = $\left\{ \begin{matrix} \text{veg. oil to ren. gas or diesel} \\ \text{sugary or starchy crop to EtOH, ren. gas or diesel} \\ \text{lignocell. crop to elec. , heat, EtOH, ren. gas or diesel} \end{matrix} \right\}$; set of 35 bioenergy pathways

$LC_{fossil}(n)$ = attrib. LC emissions from fossil fuel analog to bioenergy pathway n [$gCO_2e/MJ_{final\ energy}$]

$LC_{bio}(n)$ = attrib. LC emissions from bioenergy pathway n [$gCO_2e/MJ_{final\ energy}$]

$y(n)$ = grid cell specific areal yield of bioenergy crop n [$kg_{crop}/ha/yr$]

$c(n)$ = conversion efficiency of bioenergy crop n to final energy carrier [$MJ_{final\ energy}/kg_{crop}$]

$a(k)$ = grid cell specific area available for bioenergy crop cultivation on land type k [ha]

$\omega(n)$ = energy allocation factor of feedstock emissions to final energy carrier [%]

$LUC(k)$ = grid cell specific LUC emissions from conversion of land type k to bioenergy crop cultivation [gCO_2/ha]

m = LUC emissions amortization period [yr].

The primary energy, final energy, and specific LC emissions per unit of final energy (including LUC emissions), corresponding to bioenergy pathway n that maximizes GHG reductions, is calculated for each land use type k, in each grid cell g. Similarly, each waste and residue feedstock type (for which there are no k, $y(n)$, $a(k)$, $\omega(n)$, $LUC(k)$ or m parameters) is allocated to the conversion pathway that results in the greatest annual reduction in GHG emissions from offsetting fossil fuel use, using a simplified version of the above $R_n(k,g)$ formula.

Note that energy allocation is used at all stages of the LCA, and LUC emissions are amortized evenly over a 30-year period with no discounting (parameter m) [42]. In section 6 of the SI, we also present results assuming a 20-year amortization period [43]. The feedstock-to-fuel specific value of parameters $LC_{bio}(n)$, $c(n)$ and $\omega(n)$ are given in Table S11 of the SI.

The optimization shown in Equation 1 is performed iteratively, beginning with the value of $LC_{fossil}(n)$ intersecting with the vertical axis in Figure 2, and decreasing as the degree of final bioenergy deployment corresponds to lower LC emissions on the associated fossil fuel curve with increasing deployment of final bioenergy. This is done in increments of 5 EJ/yr of final bioenergy, requiring between 7 and 73 iterations to achieve convergence in all nine scenarios considered.

The maximum GHG emissions reduction from optimal final bioenergy deployment R_{tot} is calculated by summing all positive values of $R_n(k,g)$ over all land types k and grid cells g, given by Equation 2.

Equation 2

$$R_{tot} = \sum_{g \in [G]} \sum_{k \in [K]} R_n(k,g),$$

where

R_{tot} = total max. GHG emissions reduction from optimal final bioenergy deployment [gCO_2e/yr]

[G] = set of all grid cells

[K] $= \begin{Bmatrix} \text{pasture} \\ \text{forestland} \end{Bmatrix}$; set of all original land use types

for

$R_n(k,g) > 0$.

Payback period

Payback period is defined as the time required for the difference in LC emissions (excluding LUC emissions) between bioenergy pathway n and the fossil fuel analog to make up for a one-time pulse of LUC emissions, given by Equation 3.

Equation 3

$$PB_n(k) = \frac{\omega(n) \cdot LUC(k) \cdot a(k)}{\left[LC_{fossil}(n) \cdot y(n) \cdot c(n) \cdot a(k)\right] - \left[LC_{bio}(n) \cdot y(n) \cdot c(n) \cdot a(k)\right]},$$

where

$PB_n(k)$ payback period for bioenergy pathway n on land type k [yr].

This modeling approach is depicted schematically in Supplementary Figure 9, in order to augment the written description above.

Data availability statement

All source data used in this analysis is publically available at no charge.

In order to calculate the results presented in Figure 1, we draw on the Global Agro-ecological Zones (GAEZ) model (http://www.gaez.iiasa.ac.at) and the FAOSTAT database of historical crop yields (http://faostat3.fao.org/home/E) to estimate future energy crop yields. Arable land availability is derived from the LUH database of future land use projections (http://luh.umd.edu/), and the GTAP AEZ-EF database is used to define soil and biomass carbon stock estimates (https://www.gtap.agecon.purdue.edu/resources/res_display.asp?RecordID=4344). Additional data and description of these topics is available in Supplementary Note 1. The SSP database of population and GDP projections is used to calculate the availability of primary bioenergy feedstocks that are a function of population and economic development (https://secure.iiasa.ac.at/web-apps/ene/SspDb/dsd?Action=htmlpage&page=about#regiondefs) with additional data and description available in Supplementary Note 2. The conversion rates of bioenergy resources to final energy carriers, and the lifecycle emissions associated with them and their fossil fuel analogs, are derived from the GREET1 2015 model and database

(https://greet.es.anl.gov/greet_1_series), with additional data and description in Supplementary Note 4. Future projections of the demand for fossil fuel-derived energy carriers is from the IEA ETP (2014) database (http://www.iea.org/etp/etp2014/), with additional data and description in Supplementary Note 5.

Figures 2 and 3 are derivative of the data presented in Figure 1.

Any intermediate data not available from the sources described above, and not included in this Article or its Supplementary Notes, is available from the authors upon request.

References

1. US DOE BETO (2015) About the Bioenergy Technologies Office: growing America's energy future. Available at: http://energy.gov/eere/bioenergy/about-bioenergy-technologies-office-growing-americas-energy-future [Accessed January 13, 2016].

2. EC (2014) State of play on the sustainability of solid and gaseous biomass used for electricity, heating and cooling in the EU. (European Commission, Brussels) Available at: https://ec.europa.eu/energy/en/topics/renewable-energy/biomass [Accessed January 13, 2016].

3. IPCC (2014) IPCC task force on national greenhouse gas inventories (TFI), general guidance and other inventory issues. Available at: http://www.ipcc-nggip.iges.or.jp/faq/faq.html [Accessed January 6, 2016].

4. Wang M, Wu M, Huo H (2007) Life-cycle energy and greenhouse gas emission impacts of different corn ethanol plan types. *Environ Res Lett* 2(2): 024001.

5. Huo H, Wang M, Bloyd C, Putsche V (2009) Life-cycle assessment of energy use and greenhouse gas emissions of soybean-derived biodiesel and renewable fuels. *Environ Sci Technol* 43(3): 750-756.

6. Farrell AE et al. (2006) Ethanol can contribute to energy and environmental goals. *Science* 311: 506-508.

7. Stratton RW, Wong HM, Hileman JI (2011) Quantifying variability in life cycle greenhouse gas inventories of alternative middle distillate transportation fuels. *Environ Sci Technol* 45(10): 4637-4644.

8. Wang M, Han J, Cai H, Elgowainy A (2012) Well-to-wheels energy use and greenhouse gas emissions of ethanol from corn, sugarcane and cellulosic biomass for US use. *Environ Res Lett* 7(4): 045905.

9. Staples MD et al. (2014) Lifecycle greenhouse gas footprint and minimum selling price of renewable diesel and jet fuel from fermentation and advanced fermentation production technologies. *Energy Environ Sci* 7(5): 1545-1554.

10. Edwards R et al. (2014) JEC w*ell-to-wheels analysis: well-to-wheels analysis of future automotive fuels and powertrains in the European context.* (European Commission Joint Research Centre, Ispra, Italy) Available at: http://iet.jrc.ec.europa.eu/about-

jec/sites/iet.jrc.ec.europa.eu.about-jec/files/documents/wtw_report_v4a_march_2014_final_333_rev_140408.pdf [Accessed August 21, 2016].

11. Elgowainy A et al. (2010) *Well-to-wheels analysis of energy use and greenhouse gas emissions of plug-in hybrid electric vehicles.* (Argonne National Laboratory, Lemont IL) Available at: http://www.transportation.anl.gov/pdfs/TA/629.pdf [Accessed September 3, 2015].

12. Burnham A et al. (2012) Life-cycle greenhouse gas emissions of shale gas, natural gas, coal and petroleum. *Environ Sci Technol* 46(2): 619-627.

13. Searchinger et al. (2008) Use of US croplands for biofuels increases greenhouse gases through emissions from land-use change. *Science* 319(5867): 1238-1240.

14. Hertel etl al. (2010) Effects of US maize ethanol on global land use and greenhouse gas emissions: estimating market-mediated responses. *BioScience* 60(3): 223-231.

15. Plevin et al. (2010) Greenhouse gas emissions from biofuels' indirect land use change are uncertain but may be much greater than previously estimated. *Environ Sci Technol* 44(21): 8015-8021.

16. Fischer G, Schrattenholzer L (2001) Global bioenergy potentials through 2050. *Biomass Bioenergy* 20(3): 151-159.

17. Hoogwijk M, Faaij A, Eickhout B, de Vries B, Turkenburg W (2005) Potential of biomass energy out to 2100, for four IPCC SRES land-use scenarios. *Biomass Bioenergy* 29: 225-257.

18. Field CB, Campbell JE, Lobell DB (2008) Biomass energy: the scale of the potential resource. *Trends in Ecology & Evolution* 23(2): 65-72.

19. Ros J, Olivier J, Notenboom J, Croezen H, Bergsma G (2012) *Sustainability of biomass in a bio-based economy*. (PBL Netherlands Environmental Assessment Agency, The Hague, NL) Available at: http://www.pbl.nl/sites/default/files/cms/publicaties/PBL-2012-Sustainability-of-biomass-in-a-BBE-500143001_0.pdf [Accessed August 22, 2016].

20. Searle S, Malins C (2015) A reassessment of global bioenergy potential in 2050. *GCB Bioenergy* 7: 328-336.

21. Slade R, Bauen A, Gross R (2014) Global bioenergy resources. *Nat Clim Chang* 4(2): 99-105.

22. IEA (2014) *Energy Technology Perspectives 2014.* (OECD/IEA, Paris) Available at: http://www.iea.org/etp/etp2014/ [Accessed September 3, 2015].

23. FAOSTAT (2016) Global arable land area and area harvested. (Rome) Available at: http://fenix.fao.org/faostat/beta/en/#data/RL [Accessed October 11, 2016].

24. Daioglou V, Stehfest E, Wicke B, Faaij A, van Vuuren DP (2015) Projections of the availability and cost of residues from agriculture and forestry. *Glob Change Biol Bioenergy* Accepted for publication and available at doi: 10.1111/gcbb.12285

25. IEA (2015) CO2 emissions from fuel combustion: highlights. (OECD/IEA, Paris) Available at: http://www.iea.org/publications/freepublications/publication/CO2EmissionsFromFuelCombustionHighlights2015.pdf [Accessed August 20, 2016].

26. Trivedi P, Malina R, Barrett SRH (2015) Environmental and economic tradeoffs of using corn stover for liquid fuels and power production. *Energy Environ Sci* 8(5): 1428-1437.

27. Steubing B, Zah R, Ludwig C (2012) Heat, electricity or transportation? The optimal use of residual and waste biomass in Europe from and environmental perspective. *Environ Sci Technol* 46(1): 164-171.

28. Campbell JE, Lobell DB, Field CB (2009) Greater transportation energy and GHG offsets from bioelectricity than ethanol. *Science* 324(5930): 1055-1057.

29. IEA (2012) *Technology roadmap: bioenergy for heat and power.* (OECD/IEA, Paris) Available at: http://www.iea.org/publications/freepublications/publication/technology-roadmap-bioenergy-for-heat-and-power-.html [Accessed September 3, 2015].

30. EEA (2008) *Maximising the environmental benefits of Europe's bioenergy potential.* (EEA, Copenhagen) Available at: http://www.eea.europa.eu/publications/technical_report_2008_10 [Accessed September 3, 2015].

31. Dray L, Evans A, Reynolds T, Schaefer A (2010) Mitigation of aviation emissions of carbon dioxide. *Transp Res Rec* 2177: 17-26.

32. Hileman J, De la Rosa Blanco E, Bonnefoy PA, Carter NA (2013) The carbon dioxide challenge facing aviation. *Prog Aerosp Sci* 63: 84-95.

33. Sgouridis S, Bonnefoy PA, Hansman RJ (2011) Air transportation in a carbon constrained world: long-term dynamics of policies and strategies for mitigating the carbon footprint of commercial aviation. *Transp Res Part A Policy Pract* 45(10): 1077-1091.

34. Lal R (2008) Carbon sequestration. *Philos Trans R Soc Lond B Biol Sci* 363: 815-830.

35. Hileman JI et al. (2009) *Near-term feasibility of alternative jet fuels* (RAND Corporation, Santa Monica, CA) Available at: http://www.rand.org/pubs/technical_reports/TR554.html [Accessed September 3, 2015].

36. Bond JQ et al. (2014) Production of renewable jet fuel range alkanes and commodity chemicals from integrated catalytic processing of biomass. *Energy Environ Sci* 7: 1500-1523.

37. Cox K, Renouf M, Dargan A, Turner C, Klein-Marcuschamer D (2014) Environmental life cycle assessment (LCA) of aviation biofuels from microalgae, Pongamia pinnata, and sugarcane molasses. *Biofuel Bioprod Bior* 8: 579-593.

38. Fan J, Shonnard DR, Kalnes TN, Johnsen PB, Rao S (2013) A life cycle assessment of pennycress (Thlaspi arvense L.) –derived jet fuel and diesel. *Biomass Bioenergy* 55: 87-100.

39. Seber G, Malina R, Pearlson MN, Olcay H, Hileman JI, Barrett SRH (2014) Environmental and economic assessment of producing hydroprocessed jet and diesel fuel from waste oils and tallow. *Biomass Bioenergy* 67: 108-118.

40. Shonnard DR, Williams L, Kalnes TB (2010) Camelina-derived jet fuel and diesel: sustainable advanced biofuels. *Environ Prog Sustain Energy* 29: 382-392

41. Pearlson MN, Wollersheim CW, Hileman JI (2013) A techno-economic review of hydroprocessed renewable esters and fatty acids for jet fuel production. *Biofuel Bioprod Bior* 7: 89-96.

42. US EPA (2010) Regulation of fuels and fuel additives: changes to renewable fuel standard program; final rule. *Federal register*. 40 CFR Part 80, pp. 14669-15320.

43. EU EC (2009) Directive 2009/28/EC of the European Parliament and of the Council of 23 April 2009 on the promotion of the use of energy from renewable sources and amending and subsequently repealing Directives 2001/77/EC and 2003/30/EC. Document 32009L0028, Procedure2008/0016/COD.

44. Langeveld JWA, Dixon J, van Keulen H, Quist-Wessel PMF (2014) Analyzing the effect of biofuel expansion on land use in major producing countries: evidence of increased multiple cropping. *Biofuel Bioprod Bior* 8: 49-58.

45. Wigmosta MK, Coleman AM, Skaggs RJ, Huesemass MH, Lane LJ (2011) National microalgae biofuel production potential and resource demand. *Water Resources Research* 47(3): 1-13.

46. Rose SK, Kriegler E, Bibas R, Calvin K, Popp A, van Vuuren DP, Weyant (2014) Bioenergy in energy transformation and climate management. *Clim Change* 123(3): 477-493.

47. Humpenoeder F et al. (2014) Investigating afforestation and bioenergy CCS as climate change mitigation strategies. *Environ Res Lett* 9(6): 1-13.

48. Azar C, Johansson DJA, Mattsson N (2013) Meeting global temperature targets – the role of bioenergy with carbon capture and storage. *Environ Res Lett* 8(3): 1-8.

49. Myhre G et al. (2013) Anthropogenic and natural radiative forcing. *Climate change 2013: The physical science basis. Contribution of working group I to the Fifth Assessment Report of the Intergovernmental Panel on Climate Change,* eds Stocker, TF, Qin D, Plattner GK, Tignor M, Allen SK, Boschung J, Nauels A, Xia Y, Bex V, Midgley PM (Cambridge University Press, Cambridge UK) pp. 659-740.

50. FAOSTAT (2016) Database of historical areal crop yields. (Rome) Available at: http://faostat3.fao.org/home/E [Accessed August 20, 2016]

51. IIASA (2016) Global agro-ecological zones (GAEZ) model. (Laxenburg, Austria) Available at: http://www.gaez.iiasa.ac.at/ [Accessed August 20, 2016]

52. University of Maryland (2016) Land use harmonization project of future land use projections. (College Park, Maryland) Available at: http://luh.umd.edu/ [Accessed August 20, 2016]

53. Gibbs H, Yui S, Plevin R (2014) *New estimates of soil and biomass carbon stocks for global economic models.* (GTAP Technical Paper No. 33, Purdue University, West Lafayette, Indiana) Available at: https://www.gtap.agecon.purdue.edu/resources/download/6688.pdf [Accessed September 3, 2015]

54. IIASA (2016) SSP Database. (Laxenburg, Austria) Available at: https://secure.iiasa.ac.at/web-apps/ene/SspDb/dsd?Action=htmlpage&page=about#regiondefs [Accessed August 20, 2016].

55. Lal R (2005) World crop residues production and implications of its use as a biofuel. *Environ Int* 31: 575-584.

56. Andrews SS (2006) *Crop residue removal for biomass energy production: effects on soils and recommendations* (United States Department of Agriculture – Natural Resource Conservation Service, Washington, DC) Available at: http://www.nrcs.usda.gov/Internet/FSE_DOCUMENTS/nrcs142p2_053255.pdf [Accessed September 3, 2015]

57. Pratt MR et al. (2014) Synergies between cover crops and corn stover removal. *Agric Syst* 130: 67-76.

58. Searle S, Malins C (2014) Will energy crop yields meet expectations? *Biomass Bioenergy* 65: 3-12.

59. Smeets EMW, Faaij APC (2007) Bioenergy potentials from forestry in 2050. *Clim Change* 81(3): 353-390.

60. McKeever DB (2002) *Inventories of woody residues and solid wood waste in the United States* (United States Department Agriculture – Forest Service, Forest Product Laboratory, Washington, DC) Available at: http://originwww.fpl.fs.fed.us/documnts/pdf2004/fpl_2004_mckeever002.pdf [Accessed September 3, 2015]

61. Alexandratos N, Bruinsma J (2012) *World agriculture towards 2030/2050: the 2012 revision.* (United Nations Food and Agricultural Agency, Rome, Italy) Available at: http://www.fao.org/docrep/016/ap106e/ap106e.pdf [Accessed September 3, 2015]

62. Jayathilakan K et al. (2012) Utilization of byproducts and waste materials from meat, poultry and fish processing industries: a review. *J Food Sci Technol* 49(3): 278-293.

63. Lopez DE, Mullins JC, Bruce DA (2010) Energy life cycle assessment for the production of biodiesel from rendered lipids in the United States. *Ind Eng Chem Res* 49(5): 2419-2432.

64. Niederl A, Narodoslawsky M (2006) Ecological evaluation of processes based on by-products or waste from agriculture: life cycle assessment of biodiesel from tallow and used vegetable oil. *Feedstocks for the Future*, eds Bozell JJ, Patel MK (American Chemical Society, Washington DC), pp. 239-252.

65. The Greenhouse Gases, Regulated Emissions, Energy Use in Transportation Model (GREET 1 2015). (Argonne National Laboratory, Lemont, IL) Available at: https://greet.es.anl.gov/greet_1_series [Released October 2, 2015].

66. IEA (2014) *World Energy Outlook 2014*. (OECD/IEA, Paris) Available at: https://www.iea.org/bookshop/477-World_Energy_Outlook_2014 [Accessed September 3, 2015].

Acknowledgments

Financial support for this work was provided in part by the Natural Sciences and Engineering Research Council of Canada (NSERC), application number PGSD3-454375-2014, and in part by the Martin Family Society of Fellows for Sustainability. Any opinions, findings, and conclusions or recommendations expressed in this material are those of the authors and do not necessarily reflect the views of NSERC or the Martin Family Society. The authors wish to acknowledge Professor Wallace Tyner of Purdue University for his assistance with the GTAP AEZ-EF database, and Dr. James Hileman and Mr. Daniel Williams of the US Federal Aviation Administration for their comments on this work.

Author contributions

All three authors contributed equally to the conception and design of this work, interpretation of the results, and editing of the text. M.D.S. performed the analysis and drafted the manuscript.

Competing financial interests

The authors declare no competing financial interests.